T-helper cell diversity in experimental autoimmune encephalomyelitis and Multiple Sclerosis

Kevin S. Carbajal[*], **Yevgeniya Mironova**[†,‡], **Justin T. Ulrich-Lewis**[*], **Deven Kulkarni**[*], **Heather M. Grifka-Walk**[*,§], **Amanda K. Huber**[*], **Peter Shrager**[¶], **Roman J. Giger**[†,‡], and **Benjamin M. Segal**[*,§,‖]

[*]Holtom-Garrett Program in Neuroimmunology, Department of Neurology, University of Michigan, Ann Arbor, Michigan, USA

[†]Department of Cell and Developmental Biology, University of Michigan, Ann Arbor, Michigan, USA

[‡]Cellular and Molecular Biology Graduate Program, University of Michigan, Ann Arbor, Michigan, USA

[§]Graduate Program in Immunology, University of Michigan, Ann Arbor, Michigan, USA

[¶]Department of Neurobiology and Anatomy, University of Rochester Medical Center, Rochester, New York, USA

[‖]Neurology Service, VA Ann Arbor Healthcare System, Ann Arbor, Michigan, USA

Abstract

Multiple sclerosis (MS) is believed to be initiated by myelin-reactive $CD4^+$ Th cells. IL-12 polarized Th1 cells, IL-23 polarized Th17 cells, and exTh17 cells (Th17 cells that acquire Th1 characteristics) have each been implicated in autoimmune pathogenesis. It is currently debated whether Th cells that can drive the development of demyelinating lesions are phenotypically diverse or arise from a single lineage. In the current study we assess the requirement of IL-12 or IL-23 stimulation, as well as Th plasticity, for the differentiation of T cells capable of inducing CNS axon damage. We found that stable murine Th1 and Th17 cells independently transfer experimental autoimmune encephalomyelitis (EAE, widely used as an animal model of MS) in the absence of IL-23 and IL-12, respectively. Plastic Th17 cells are particularly potent mediators of demyelination and axonopathy. In parallel studies, we identified MS patients who consistently mount either IFNγ- or IL-17- skewed responses to myelin basic protein (MBP) over the course of a year. Brain magnetic resonance imaging revealed that patients with mixed IFNγ and IL-17 responses have relatively high T1 lesion burden, a measure of permanent axon damage. Our data challenge the dogma that IL-23 and Th17 plasticity are universally required for the development of EAE. This study definitively demonstrates that autoimmune demyelinating disease can be driven by distinct Th polarizing factors and effector subsets, underscoring the importance of a customized approach to the pharmaceutical management of MS.

Address correspondence to: Benjamin M. Segal, 4013 BSRB, Ann Arbor, Michigan, 48109, USA. Phone: 734.615.5635; Fax: 734.615.0036; bmsegal@umich.edu.

Keywords

EAE/MS; Cytokines; Neuroimmunology; Human; Rodent; T Cells

Introduction

Multiple sclerosis (MS) is widely believed to be an autoimmune disease mediated by $CD4^+$ T cells reactive against myelin antigens. Significant advances have been made in the development of immunomodulatory agents that decrease MS relapse rates. However, none of those agents target encephalitogenic T cells while sparing protective immune responses. An increased understanding of the factors that drive the differentiation and function of myelin-reactive T cells would help guide the development of more refined therapeutic modalities. IFNγ-producing $CD4^+$ T cells of the Th1 lineage were initially thought to be the critical effector cells in MS and the animal model, experimental autoimmune encephalomyelitis (EAE) [1, 2]. The putative role of Th1 cells in EAE was buttressed by the finding that *in vitro* stimulation of ordinarily innocuous myelin-reactive $CD4^+$ T cells with the Th1 polarizing factor IL-12, could confer encephalitogenicity [3]. Furthermore, C57BL/6 mice deficient in the Th1 associated transcription factor, T-bet, have a decreased incidence of EAE following immunization with an epitope of myelin oligodendrocyte glycoprotein (MOG_{35-55}) [4]. However, a universal role of Th1 effectors in autoimmune demyelination was challenged by the discovery that IL-17 producing Th17 cells also accumulate in EAE and MS lesions and can transfer EAE [5, 6]. Actively immunized C57BL/6 mice that are deficient in the Th17 polarizing factor, IL-23, are completely EAE resistant, and those deficient in the Th17 associated transcription factor, RORγt, are partially resistant [7, 8].

In an attempt to reconcile these data, others and we have argued that EAE and MS are heterogeneous disorders, and that the importance of specific leukocyte subsets and/or proinflammatory factors in disease development is context-dependent [9, 10]. A link between Th17 and Th1 mediated autoimmunity was revealed by the demonstration that some Th17 cells are plastic and acquire Th1-like characteristics after several rounds of activation [11]. These "exTh17" cells downregulate IL-17 and RORγt, and upregulate IFNγ and T-bet. Fate mapping experiments demonstrated that exTh17 cells comprise the majority of $CD4^+$ lymphocytes that infiltrate the CNS in MOG_{35-55}-immunized C57BL/6 mice [12]. Although this observation has prompted some investigators to portray myelin-specific exTh17 cells as the critical effectors in EAE, the relative capacities of Th1, stable Th17 and plastic Th17 cells to induce demyelination and axonopathy have not been directly tested. Here we interrogate the contributions of IL-12 and IL-23 signaling, as well as Th plasticity, to the acquisition of encephalitogenic properties by myelin-reactive T cells. In parallel, we conducted a longitudinal study to investigate myelin-specific cytokine profiles of patients with MS.

Materials and Methods

Mice

Eight- to 12-week-old C57BL/6 and CD45.1 congenic C57BL/rsLy5.2/Cr mice were obtained from NCI Frederick (Frederick, MD, USA). C57BL/6 *IL12p35*$^{−/−}$ mutant mice were obtained from Jackson Laboratory (Bar Harbor, ME) and subsequently bred in our facility. *IL23p19*$^{−/−}$ mutant mice backcrossed on a C57BL/6 background have previously been described [13]. All mice were housed in micro-isolator cages under specific pathogen-free, barrier facility conditions.

Induction of EAE by adoptive transfer

Donor mice were anesthetized with Avertin (Sigma) and injected subcutaneously with MOG$_{35-55}$ (100 μg, Biosynthesis) emulsified in CFA containing 400 mg/ml of heat-killed *Mycobacterium tuberculosis* H37Ra, Difco). Ten to 14 days post-immunization, a single-cell suspension was prepared from pooled draining inguinal, axillary, and brachial lymph nodes (LNs) and passed through a 70 μm cell strainer (BD Falcon). LN cells were cultured *in vitro* for 4 days with MOG$_{35-55}$ under conditions favorable to the generation of Th1 cells (rmIL-12, 6 ng/mL; rmIFN-γ, 2 ng/mL; anti-IL-4 (clone 11B11), 10 μg/mL) or Th17 cells (rmIL-1α, 10 ng/mL; rmIL-23, 8 ng/mL; anti-IL-4, 10 μg/mL; anti-IFN-γ (clone XMG1.2) 10 μg/mL). After 4 days culture, LN cells were collected, washed and injected into naïve syngeneic recipients (2×10^6 CD4$^+$ T cells/mouse). Adoptive transfer recipients were monitored daily for neurological deficits and rated using the following criteria: 1, hypotonic and weak tail; 2, waddling gait and difficulty righting; 3, overt hindlimb weakness; 4, hindlimb paralysis; 5, moribund.

Flow cytometry

Brains, spinal cords and optic nerves were harvested at serial time points following the onset of neurological deficits (1–2, 5–6 and 21–22 days post-onset), homogenized in DNase (1 mg/mL) and collagenase A (2 mg/mL) and incubated for 30 min at 37 °C. Mononuclear cells were then isolated over a 30/70% Percoll gradient (GE Healthcare). Splenocytes were passed through a 70 μm cell strainer, ACK lysed and washed twice. For intracellular staining, cells were stimulated with PMA (50 ng/mL) and ionomycin (2 μg/mL) in the presence of brefeldin A (10μg/mL) for 6 hours. Cells were fixed with 4% paraformaldehyde and permeabilized with 0.5% saponin prior to incubation with flourochrome-conjugated antibodies. Flow cytometry was performed using a BD FacsCanto II and data were analyzed using FlowJo (Tree Star Inc.). All plots are gated from live, CD45$^+$ singlets. CD4$^+$ T cells are further gated on CD3$^+$ counts.

Antibodies and reagents

The following antibodies were used for flow cytometry or immunohistochemistry: rat anti-MBP (Millipore); mouse anti-unphosphorylated neurofilament-H (SMI-32, Covance); CD45 (Serotec), Brn3a (Santa Cruz); Alexa Fluor 594 goat anti-mouse IgG and Alexa Fluor 488 goat anti-rat IgG (Life Technologies); FITC–anti-MHCII, FITC–anti-B220, PE–anti-CD45 (Ly5), PE–anti-CD8α, PE–anti-CD4, PE–anti–GM-CSF, PECy7–anti-CD11b, and PECy7–

anti-CD4; PerCpCy5.5–anti-Ly6C, PerCPCy5.5–anti-CD3ε, and PerCPCy5.5–anti–IL-17A (e-Bioscience); BD Biosciences: allophycocyanin–anti-CD45.2, FITC–anti-CD44, allophycocyanin cy7–anti-Ly6G, allophycocyanin cy7–anti-CD45.1, and allophycocyanin cy7–anti–IFN-γ (BD Biosciences). Recombinant mouse (rm) IFN-γ, IL-23 and rmIL-12 were from R&D Systems.

Histology

Eyes and optic nerves were harvested, fixed in 4% paraformaldehyde (PFA), and cryoprotected in 30% sucrose. Specimens were embedded in OCT Tissue-Tek Medium (Sakura Finetek) and cut into 12 μm (nerves) or 20 μm (eyes) sections on a Thermo Scientific Microm HM550 cryostat. Immunofluorescent staining was performed with primary antibodies against CD45 (1:100), Brn3a (1:200) and SMI-32 (1:1000). Citrate buffer antigen retrieval was performed for SMI-32 staining. Goat anti-mouse IgG Alexa Fluor 594 (1:500) and goat anti-rat IgG Alexa Fluor 488 (1:500) were used as secondary antibodies. Sections were incubated with DAPI (100 ng/ml) prior to washing and mounting on slides (Prolong Gold Antifade Reagent, Life Technologies). Fluorescent images were acquired with a Nikon Eclipse Ti, CoolSnapEZ camera, and NIS Elements: Basic Research v3.10. Confocal images were acquired using a Nikon A-1 Confocal microscope (Nikon Plan Fluor 10×/0.30 or Nikon Plan ApoVC 60×/1.40 oil) with diode-based laser system and NIS Elements software. Three-dimensional reconstruction images were constructed from confocal Z-stack images using Bitplane software (Imaris). Additional image processing was performed with Adobe Photoshop CS5.1 and applied equally to all samples and controls. For tracing studies, anesthetized (Avertin) mice received intravitreal injections (2 μl) of 1 μg μl^{-1} Alexa 594–conjugated cholera toxin β (Invitrogen) in both eyes. Mice were euthanized 24 hours post-injection and their optic nerves were dissected, post-fixed in 4% paraformaldehyde overnight and cryoprotected in 30% sucrose.

Quantification of histological parameters

Brn3a-positive cells were counted in the ganglion cell layer in four to nine cross-sections of the entire retina perpendicular to the corneoscleral divide. Contiguous longitudinal sections of optic nerves (from the nerve head to the chiasm) were stained for CD45 or SMI32. Swollen SMI32$^+$ axons were manually counted in 500 μm long segments. The mean fluorescence intensity of CD45 staining was measured in the corresponding segment using Image J. Total SMI32$^+$ axons were enumerated in three or more coronal sections per nerve, approximately 1 mm proximal to the chiasm.

Electrophysiology

Optic nerve recording of compound action potentials (CAPs) was performed as described previously [14]. Nerves were harvested at the same time following onset but before peak of disease. Four nerves were measured per group per each of three to four independent experiments. Briefly, mice were euthanized with CO_2 and optic nerves were dissected and incubated in artificial cerebrospinal fluid, containing (mM): NaCl 125, NaH_2PO_4 1.25, glucose 25, $NaHCO_3$ 25, $CaCl_2$ 2.5, $MgCl_2$ 1.3, KCl 2.5 and saturated with 95% O_2/5% CO_2. Nerves were drawn into suction electrodes for stimulation and recording at 37 °C. Signals were amplified and acquired with a Digidata 1440A under Clampex software (Axon

instruments). Analysis was performed offline using Clampfit. Amplitude and conduction velocity values for individual components of the CAP were derived by fitting with multiple Gaussians using Origin Pro [15]. Statistical analysis was performed with Microsoft Excel and Graphpad Prism.

Multiple Sclerosis Subjects

Patients diagnosed with relapsing MS (n=36) based on the revised McDonald Diagnostic Criteria [16] were recruited from the Multiple Sclerosis Clinics at the University of Michigan and the University of Rochester. All subjects had a moderate degree of disability (EDSS score 2.5–4.5) and none were treated with disease modifying therapies.

ELISPOT Assays

PBMCs were obtained from study participants on a monthly basis over the course of 1 year. PBMCs were isolated using CPT Vacutainer tubes (Fisher Scientific), suspended in fetal bovine serum with 20% dimethyl sulfoxide, and stored in liquid nitrogen until thawed for analysis. ELISPOT assays were performed to enumerate the frequencies of MBP-specific IFNγ and IL-17 producers, using a protocol that we previously described [17]. Subjects were classified as IFNγ-skewed if the frequency of MBP-specific IFNγ producers in their PBMC exceeded that of IL-17 producers by two-fold or more in at least two thirds of samples. Conversely, IL-17-skewed subjects had twice or greater the frequency of MBP-specific IL-17 producers than IFNγ-producers in at least two thirds of PBMC samples. Subjects who did not meet either of the above criteria were classified as mixed.

MRI protocol and imaging analysis

All patients were evaluated by cranial MRI examination on a 1.5 Tesla-strength magnet using axial T2-weighted and axial and sagittal T1-weighted sequences. Brain parenchymal and T1 and T2 lesion volumes were measured using commercial software developed by VirtualScopics (Rochester, NY) as previously described [17].

Statistics

Analyses were performed using GraphPad Prism software. Leukocyte cell numbers and percentages were compared using the unpaired Student t-test. Axon counts were analyzed by one-way ANOVA and electrophysiological recordings by the Mann-Whitney test. MRI lesion volumes were analyzed with one-way ANOVA (Kruskal-Wallis) and Dunn's multiple comparisons test. $P<0.05$ (*) was considered significant.

Study approval

All EAE experiments were performed in compliance with local and national animal care guidelines and approved by the University of Michigan Committee on Use and Care of Animals. The Institutional Review Boards of the University of Michigan and the University of Rochester approved our human study protocol. Informed consent was obtained from each subject.

Results

Characteristics of Optic Nerve Inflammation in Th1 and Th17 adoptive transfer recipients

We have previously shown that the clinical course of EAE is comparable between C57BL/6 mice injected with IL-12- or IL-23-polarized, MOG_{35-55}-reactive Th1 and Th17 cells, respectively [9, 10, 18]. The same T cells activated under neutral conditions do not induce CNS infiltrates or clinical EAE. In preliminary experiments, we performed flow cytometric analyses of optic nerves and spinal cords harvested from Th1 and Th17 adoptive transfer recipients at serial time points. The majority of host mice (<90%) had bilateral optic neuritis (ON) on the day of onset of clinical EAE, irrespective of donor Th phenotype (unpublished data). A significant percent of IL-12 polarized donor T cells produced IFNγ immediately prior to transfer, as well as in host spinal cords and optic nerves (Fig. 1A and B). In contrast, intracellular IL-17 staining rarely exceeded background levels. As expected, a high percent of IL-23 polarized T cells expressed IL-17, both prior to, and following, adoptive transfer. However, there were significant subpopulations of IL-17/IFNγ double producers and IFNγ single producers among IL-23 polarized donor cells harvested after 96 hours of culture, consistent with transition into ex-Th17 cells (Fig. 1A). The percent of IFNγ single producers within the CNS of mice injected with IL-23 polarized T cells equaled or exceeded the percent of IL-17 single producers (Fig. 1B). Consistent with prior publications, high percentages of infiltrating CD4+ T cells produced GM-CSF, irrespective of Th lineage (Fig 1B) [19–21]. In both Th1 and Th17 adoptive transfer recipients, the cellular composition of CNS mononuclear cells and cytokine profile of infiltrating T cells were comparable in the optic nerve and spinal cord (Fig. 1B and C). Hence, in subsequent experiments we focused on the pathology of optic nerves, due to their accessibility for axonal tracing and electrophysiological studies.

Morphological and ultrastructural abnormalities in inflamed optic nerves of mice with Th1- and Th17-mediated disease

Although MS has previously been characterized as a primary demyelinating disorder, axonal transections and swellings are pervasive features of the disease, and axonal loss correlates with disability [22–24]. The relative contribution of myelin-reactive Th1 and Th17 cells to axonopathy has yet to be assessed. We detected axonal swellings in recipients of both IL-12 and IL-23 polarized T cells shortly following clinical EAE onset (Fig. 2A and 2B). Confocal microscopy demonstrated that some of the swellings were located at the tips of transected axons (Fig. 2C). These swellings were also apparent in sections stained for unphosphorylated neurofilament-H (SMI-32) (Fig. 2E–G). Demyelination was evident in areas of inflammation early in the clinical course. However, we frequently observed swollen or degenerating axons surrounded by myelin, suggesting that axonopathy can occur without overt myelin damage (Fig. 2H–J, and data not shown). Similar to other regions of the CNS, inflammation of the optic nerve is multifocal and discontinuous in mice with EAE (Fig. 2A and B). The frequency of axonal swellings correlated with staining for the pan-leukocyte marker CD45, a measure of inflammation (Fig. 2D). The relationship between axonal swellings and inflammation was comparable in IL-I2- and IL-23-mediated ON. Optic nerve axon loss was already apparent in both groups of transfer recipients at clinical presentation (Fig. 3A–D). The number of retinal ganglion cells (RGC), the neurons that give rise to optic

nerve axons, was reduced at chronic, but not earlier time points (Fig. 3E). There were no significant differences in the extent of axon or RGC loss between groups of mice with ON (Fig. 3D and E).

Conduction deficits in optic nerves of mice with Th1- and Th17-mediated EAE

EAE lesions are heterogenous with regard to location, volume and severity of damage. Quantification of myelin breakdown across multifocal lesions via histological or immunohistochemical techniques is challenging and prone to sampling error. Furthermore, the relative contributions of demyelination and axonopathy to disability cannot be measured by those approaches. To overcome these limitations, we performed functional studies by subjecting acutely isolated optic nerves from Th1 and Th17 adoptive transfer recipients to electrophysiological recordings. We measured velocities and amplitudes of compound action potentials (CAPs) at disease onset. A reduction in CAP amplitude is indicative of axon loss and/or conduction block, while a reduction in velocity is indicative of demyelination. CAP amplitudes and velocities of fast-, intermediate- and slow-conducting fibers (AMP1/CV1, AMP2/CV2 and AMP3/CV3, respectively) were all reduced in both groups of transfer recipients compared with naïve mice (Fig. 3F–J).

Stable Th17 cells are capable of inducing ON

ExTh17 cells have been portrayed as the critical effector cells in autoimmune demyelinating disease. Conversion of Th17 cells into exTh17 cells is promoted by IL-12 [11]. In order to determine whether plasticity contributes to the acquisition of encephalitogenic properties by Th17 cells, we polarized CD4$^+$ T cells from MOG-primed IL-12 deficient (IL-12KO) donors with antigen and recombinant IL-23. After 96 hours of culture, a relatively high percent of those cells expressed IL-17 (Fig. 4. A). Unlike primed wild-type (WT) cells cultured under Th17 polarizing conditions (Fig. 1A), MOG-reactive CD4$^+$ T cells derived from IL-12KO donors had low frequencies of IFNγ producers *in vitro* (Fig. 4A). Furthermore, these cells maintained a Th17 phenotype after infiltrating the spinal cords and optic nerves of syngeneic IL-12KO hosts (Fig. 4B). Hence, hereafter we refer to IL-23 polarized cells from WT and IL-12KO donors as plastic and stable Th17 cells, respectively. Stable Th17 cells induced EAE with a clinical course that was indistinguishable from that induced by WT Th17 cells (Fig. 4C). Stable Th17 cells also resembled their plastic counterparts by producing GM-CSF as well as IL-17, and inducing infiltrates of similar cellular composition, in the optic nerves and spinal cord (Fig. 1B and C, 4B and D). At clinical onset, we isolated comparable numbers of CD45$^+$ cells from the optic nerves of hosts injected with stable or plastic Th17 effectors (data not shown). Reminiscent of our findings with plastic Th17 cells, stable Th17 cells induced axonal swellings and demyelination in the optic nerves of adoptive transfer recipients at early time points (Fig. 4E and F). This was corroborated by electrophysiological studies, which showed significant reductions in CAP amplitudes and velocities compared with naïve IL-12KO controls (Fig. 4G–I). The reduction in CAP velocities induced by stable Th17 cells was modest when compared to the degree of slowing induced by plastic Th17 cells (Fig. 3G, 4H). Plastic Th17 cells were also more effective in reducing the CAP amplitudes of fast conducting fibers (Fig. 3H and 4I). These observations could reflect an enhanced pathogenicity of exTh17 cells compared with stable Th17 cells. Alternatively, Th1 cells might contaminate the pool of IL-23 stimulated WT donor cells and

act synergistically with Th17 cells to induce inflammatory infiltration and CNS tissue damage [25].

Bona fide Th1 cells can induce EAE in the absence of IL-23

We next questioned whether Th1 cells are capable of inducing EAE independent of stable Th17 cells and/or exTh17 cells. Since the IL-12 polarized T cells used in our earlier experiments were derived from WT donors, it is possible they were contaminated with exTh17 cells that had been exposed to IL-23 during priming *in vivo*. To generate a pure population of "bona fide" Th1 cells, we primed IL-23KO donors with MOG_{35-55} in CFA, and cultured draining lymph node cells with antigen and recombinant IL-12. $CD4^+$ T cells were then transferred into naïve syngeneic IL-23KO hosts. These Th1-polarized cells, never exposed to IL-23, produced IFNγ and GM-CSF, but no significant IL-17, pre- as well as post-transfer (Fig. 5A and B; data not shown). They induced EAE at 90–100% incidence in repeated experiments, though peak severity was slightly lower than we observed with WT to WT transfers (Fig. 5 C). Optic nerve and spinal cord infiltrates induced by IL-23KO Th1 cells had a similar cellular composition (Fig. 5D). At clinical onset, we isolated comparable numbers of $CD45^+$ cells from the optic nerves of WT and IL-12KO hosts injected with WT or IL-12KO Th1 effectors, respectively (data not shown). Bona fide Th1 cells were still capable of inducing axonal swellings and demyelination (Fig. 5E and F), and caused reductions in CAP amplitudes (Fig. 5G and I). However, they were relatively ineffective at inducing CAP slowing (Fig. 5G and H).

Anti-myelin cytokine responses in MS patients

MS is a heterogeneous disease with regard to the clinical course, extent and pattern of CNS injury, and therapeutic responsiveness to disease modifying therapy. Our EAE studies raise the question of whether autoreactive Th responses can be used to define subsets of multiple sclerosis patients that are pathophysiologically and/or clinically meaningful. As a first step in addressing that issue, we performed a longitudinal exploratory study to measure myelin basic protein (MBP)-specific IFNγ and IL-17 responses in a cohort of relapsing MS patients with moderate disability and a history of ON and myelitis. PBMC were collected on a monthly basis over the course of 1 year. The frequency of MBP-specific cytokine producing cells was quantified by ELISPOT. We found that 23% of patients consistently mounted IFNγ-skewed responses, 17% had an IL-17 dominant pattern, while the remainder had comparable or oscillating frequencies of IFNγ and IL-17 producers (Fig. 6A). Cerebral MRI scans were obtained from each subject and analyzed as previously described [17]. Average MRI T2 lesion load was similar across the three groups (Fig. 6B). T1 lesion load, which is associated with severe CNS injury and axonal loss, was relatively high in patients with the mixed IL-17/IFNγ pattern (Fig. 6C).

Discussion

The current study provides further insight into the pathophysiology of autoimmune demyelinating disease mediated by Th1 and Th17 cells. We and others have previously demonstrated that the adoptive transfer of either IL-12 or IL-23 polarized WT Th effector cells can induce EAE [9, 10]. These two forms of disease differ in CNS expression of

downstream chemokines and proinflammatory factors, and therapeutic responsiveness to immunomodulatory agents. Here we extend those findings by showing that both Th effector cell types are capable of mediating axonopathy and demyelination. We chose to focus this study on the pathology of the inflamed optic nerve due to its accessibility for anterograde tracing experiments and electrophysiological analysis. In addition to providing a functional read-out measure, electrophysiology is particularly important to assess collective tissue damage in light of the inherent challenges of quantifying multifocal axonopathy and demyelination via histological or immunohistochemical approaches. Inflammation, demyelination and axonopathy appeared qualitatively similar in optic nerves compared with the spinal cord, irrespective of Th polarizing conditions or the cytokine profile of the myelin-reactive donor T cells. Furthermore, there were no significant differences in the cellular composition of optic nerve and spinal cord infiltrates isolated from the same group of mice, based on the panel of cell surface markers we measured by flow cytometry. Nonetheless, the optic nerve has a unique anatomical structure, and only future studies will determine whether the interactions between infiltrating inflammatory cells and resident glial cells differ between CNS compartments.

Experiments that compare the properties of IL-12 and IL-23-polarized CD4$^+$ T cells derived from primed WT donors are complicated by the possibility of contamination by T cells of the alternative lineage, as well as by the plasticity of WT Th cells. The ability of myelin-reactive Th1 cells to transfer EAE has been challenged by the assertion that IL-23 signaling is universally required for the acquisition of pathogenic properties [7, 26]. It could be argued that IL-12 polarized CD4$^+$ cells, generated from MOG-primed WT donors, may be contaminated with exTh17 cells that are actually responsible for disease induction upon adoptive transfer. However, contrary to the current dogma, our data demonstrate that bona fide Th1 cells, which have never been exposed to IL-23, either during the priming or effector stages, can induce damage to axons and myelin. A related issue is whether Th17 cells become pathogenic only after transitioning into exTh1 cells [12]. Our results indicate that, while plasticity may enhance the potency of myelin-reactive Th17 cells, it is not absolutely required for the acquisition of disease causing properties.

Although stable Th17 cells, derived from IL-12 KO hosts, and bona fide Th1 cells, derived from IL-23 KO hosts, were both capable of inducing ON, they were not as effective as their WT counterparts. This was particularly evident with regard to CAP slowing. One hypothetical explanation for our results is that autoreactive ex-Th17 cells are particularly potent inducers of myelin damage and, as mentioned above, may have contributed to the IL-12-, as well as the IL-23-, polarized WT transfers. Alternatively, EAE studies suggest that Th1 and Th17 cells act synergistically in triggering neuroinflammation and downstream CNS pathology [25]. Future studies with fate mapping mice will be necessary to distinguish between those possibilities.

MS is a heterogeneous disease with regard to the clinical course, extent and pattern of CNS injury, and therapeutic responsiveness to disease modifying therapies. A clearer understanding of the mechanistic basis of this diversity will be critical for the future discovery of biomarkers and the design of customized medications. An important question broached by our study is whether differences in anti-myelin Th cell cytokine responses can

be used to define subsets of MS patients that are pathophysiologically and/or clinically meaningful. As a first step in answering that question, we found that the MS patients in our cohort exhibit a range of patterns of IFNγ and IL-17 production by MBP-reactive PBMC. Furthermore, in some patients these patterns were stable over the course of 1 year. The human studies described in this paper are exploratory, and future studies with larger independent cohorts will be necessary to determine whether immune profiles correlate with clinical, radiologic and/or histopathological manifestations of disease, or with responsiveness to individual disease modifying agents.

This study demonstrates that the autoreactive Th repertoire in CNS autoimmune disease may be skewed towards a Th1 or Th17 lineage. Our EAE experiments serve as a proof of principle that highly polarized and stable Th1 or Th17 cells are capable of inducing classical features of MS independent of the reciprocal differentiation factor. The fact that full-blown EAE can occur in the absence of IL-23, a cytokine that has been thought to play an essential role in pathogenesis, provides further evidence against a universal therapeutic target in MS. Our data underscore the importance of discovering biomarkers that define pathologically distinct subsets of individuals with MS in order to guide the design of more effective clinical trials and to facilitate the development of customized medicine in MS.

Acknowledgments

Abbreviations

CAP	compound action potential
EAE	experimental autoimmune encephalomyelitis
MBP	myelin basic protein
MOG	myelin oligodendrocyte glycoprotein
Th	T-helper
WT	wildtype

References

1. Voskuhl RR, Martin R, Bergman C, Dalal M, Ruddle NH, McFarland HF. T helper 1 (Th1) functional phenotype of human myelin basic protein-specific T lymphocytes. Autoimmunity. 1993; 15:137–143. [PubMed: 7692995]

2. Segal BM. Experimental autoimmune encephalomyelitis: cytokines, effector T cells, and antigen-presenting cells in a prototypical Th1-mediated autoimmune disease. Curr Allergy Asthma Rep. 2003; 3:86–93. [PubMed: 12543000]

3. Segal BM, Shevach EM. IL-12 unmasks latent autoimmune disease in resistant mice. J Exp Med. 1996; 184:771–775. [PubMed: 8786337]

4. Bettelli E, Sullivan B, Szabo SJ, Sobel RA, Glimcher LH, Kuchroo VK. Loss of T-bet, but not STAT1, prevents the development of experimental autoimmune encephalomyelitis. J Exp Med. 2004; 200:79–87. [PubMed: 15238607]

5. Langrish CL, Chen Y, Blumenschein WM, Mattson J, Basham B, Sedgwick JD, McClanahan T, Kastelein RA, Cua DJ. IL-23 drives a pathogenic T cell population that induces autoimmune inflammation. J Exp Med. 2005; 201:233–240. [PubMed: 15657292]

6. Kebir H, Ifergan I, Alvarez JI, Bernard M, Poirier J, Arbour N, Duquette P, Prat A. Preferential recruitment of interferon-gamma-expressing TH17 cells in multiple sclerosis. Ann Neurol. 2009; 66:390–402. [PubMed: 19810097]

7. Cua DJ, Sherlock J, Chen Y, Murphy CA, Joyce B, Seymour B, Lucian L, To W, Kwan S, Churakova T, Zurawski S, Wiekowski M, Lira SA, Gorman D, Kastelein RA, Sedgwick JD. Interleukin-23 rather than interleukin-12 is the critical cytokine for autoimmune inflammation of the brain. Nature. 2003; 421:744–748. [PubMed: 12610626]

8. Ivanov II, McKenzie BS, Zhou L, Tadokoro CE, Lepelley A, Lafaille JJ, Cua DJ, Littman DR. The orphan nuclear receptor RORgammat directs the differentiation program of proinflammatory IL-17+ T helper cells. Cell. 2006; 126:1121–1133. [PubMed: 16990136]

9. Kroenke MA, Carlson TJ, Andjelkovic AV, Segal BM. IL-12- and IL-23-modulated T cells induce distinct types of EAE based on histology, CNS chemokine profile, and response to cytokine inhibition. J Exp Med. 2008; 205:1535–1541. [PubMed: 18573909]

10. Axtell RC, de Jong BA, Boniface K, van der Voort LF, Bhat R, De Sarno P, Naves R, Han M, Zhong F, Castellanos JG, Mair R, Christakos A, Kolkowitz I, Katz L, Killestein J, Polman CH, de Waal Malefyt R, Steinman L, Raman C. T helper type 1 and 17 cells determine efficacy of interferon-beta in multiple sclerosis and experimental encephalomyelitis. Nat Med. 2010; 16:406–412. [PubMed: 20348925]

11. Lee YK, Turner H, Maynard CL, Oliver JR, Chen D, Elson CO, Weaver CT. Late developmental plasticity in the T helper 17 lineage. Immunity. 2009; 30:92–107. [PubMed: 19119024]

12. Hirota K, Duarte JH, Veldhoen M, Hornsby E, Li Y, Cua DJ, Ahlfors H, Wilhelm C, Tolaini M, Menzel U, Garefalaki A, Potocnik AJ, Stockinger B. Fate mapping of IL-17-producing T cells in inflammatory responses. Nat Immunol. 2011; 12:255–263. [PubMed: 21278737]

13. Ghilardi N, Kljavin N, Chen Q, Lucas S, Gurney AL, De Sauvage FJ. Compromised humoral and delayed-type hypersensitivity responses in IL-23-deficient mice. J Immunol. 2004; 172:2827–2833. [PubMed: 14978083]

14. Fernandes KA, Harder JM, John SW, Shrager P, Libby RT. DLK-dependent signaling is important for somal but not axonal degeneration of retinal ganglion cells following axonal injury. Neurobiol Dis. 2014; 69:108–116. [PubMed: 24878510]

15. Winters JJ, Ferguson CJ, Lenk GM, Giger-Mateeva VI, Shrager P, Meisler MH, Giger RJ. Congenital CNS hypomyelination in the Fig4 null mouse is rescued by neuronal expression of the PI(3,5)P(2) phosphatase Fig4. J Neurosci. 2011; 31:17736–17751. [PubMed: 22131434]

16. Polman CH, Reingold SC, Banwell B, Clanet M, Cohen JA, Filippi M, Fujihara K, Havrdova E, Hutchinson M, Kappos L, Lublin FD, Montalban X, O'Connor P, Sandberg-Wollheim M, Thompson AJ, Waubant E, Weinshenker B, Wolinsky JS. Diagnostic criteria for multiple sclerosis: 2010 revisions to the McDonald criteria. Ann Neurol. 2011; 69:292–302. [PubMed: 21387374]

17. Huber AK, Wang L, Han P, Zhang X, Ekholm S, Srinivasan A, Irani DN, Segal BM. Dysregulation of the IL-23/IL-17 axis and myeloid factors in secondary progressive MS. Neurology. 2014; 83:1500–1507. [PubMed: 25253754]

18. Kroenke MA, Chensue SW, Segal BM. EAE mediated by a non-IFN-γ/non-IL-17 pathway. Eur J Immunol. 2010; 40:2340–2348. [PubMed: 20540117]

19. Codarri L, Gyülvészi G, Tosevski V, Hesske L, Fontana A, Magnenat L, Suter T, Becher B. RORγt drives production of the cytokine GM-CSF in helper T cells, which is essential for the effector phase of autoimmune neuroinflammation. Nat Immunol. 2011; 12:560–567. [PubMed: 21516112]

20. El-Behi M, Ciric B, Dai H, Yan Y, Cullimore M, Safavi F, Zhang GX, Dittel BN, Rostami A. The encephalitogenicity of T(H)17 cells is dependent on IL-1- and IL-23-induced production of the cytokine GM-CSF. Nat Immunol. 2011; 12:568–575. [PubMed: 21516111]

21. Ponomarev ED, Shriver LP, Maresz K, Pedras-Vasconcelos J, Verthelyi D, Dittel BN. GM-CSF production by autoreactive T cells is required for the activation of microglial cells and the onset of experimental autoimmune encephalomyelitis. J Immunol. 2007; 178:39–48. [PubMed: 17182538]

22. Trapp BD, Peterson J, Ransohoff RM, Rudick R, Mork S, Bo L. Axonal transection in the lesions of multiple sclerosis. N Engl J Med. 1998; 338:278–285. [PubMed: 9445407]

23. Soulika AM, Lee E, McCauley E, Miers L, Bannerman P, Pleasure D. Initiation and progression of axonopathy in experimental autoimmune encephalomyelitis. J Neurosci. 2009; 29:14965–14979. [PubMed: 19940192]

24. De Stefano N, Matthews PM, Fu L, Narayanan S, Stanley J, Francis GS, Antel JP, Arnold DL. Axonal damage correlates with disability in patients with relapsing-remitting multiple sclerosis. Results of a longitudinal magnetic resonance spectroscopy study. Brain. 1998; 121(Pt 8):1469–1477. [PubMed: 9712009]

25. O'Connor RA, Prendergast CT, Sabatos CA, Lau CW, Leech MD, Wraith DC, Anderton SM. Cutting edge: Th1 cells facilitate the entry of Th17 cells to the central nervous system during experimental autoimmune encephalomyelitis. J Immunol. 2008; 181:3750–3754. [PubMed: 18768826]

26. Becher B, Durell BG, Noelle RJ. IL-23 produced by CNS-resident cells controls T cell encephalitogenicity during the effector phase of experimental autoimmune encephalomyelitis. J Clin Invest. 2003; 112:1186–1191. [PubMed: 14561703]
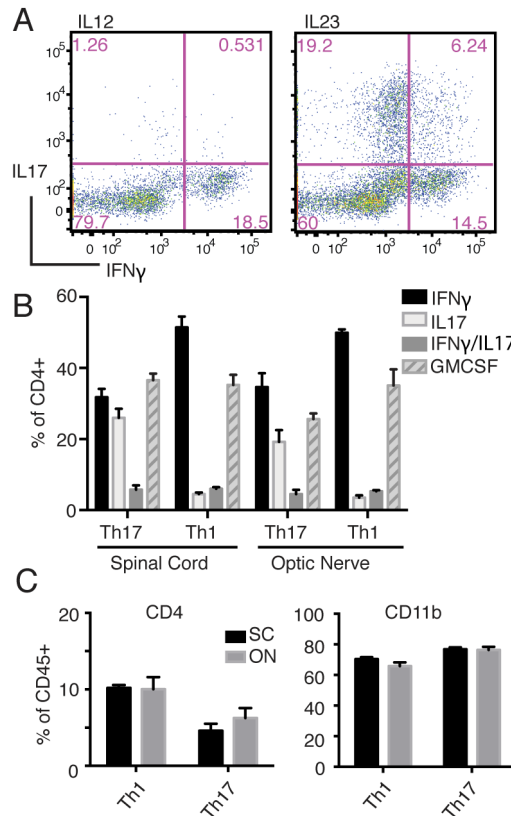
FIGURE 1.
IL-12 and IL-23 polarized CD4$^+$ T cells are both capable of mediating ON. (**A-C**) C57BL/6 mice were immunized with MOG$_{35-55}$ emulsified in CFA. Ten to fourteen days later, draining lymph node cells were harvested and cultured for 96 hours with MOG$_{35-55}$ and either recombinant IL-12 or IL-23 to generate Th1 and Th17 cells, respectively. (**A**) Intracellular staining and flow cytometric analysis of cultured cells at 96 hours, gating on the CD3$^+$CD4$^+$ population. (**B, C**) Following culture, CD4$^+$ T cells were transferred into naïve syngenic recipients. Mice in each group were euthanized at day 9 post-transfer, the day after clinical EAE onset. Mononuclear cells isolated from optic nerves (ON) and spinal cords (SC) were assessed for CD4$^+$ T cell cytokine production (**B**) and the percent of CD4$^+$ T cells and CD11b$^+$ myeloid cells among CD45$^+$ leukocytes (**C**) by flow cytometry. Data are representative of three independent experiments with at least 3 mice per group.
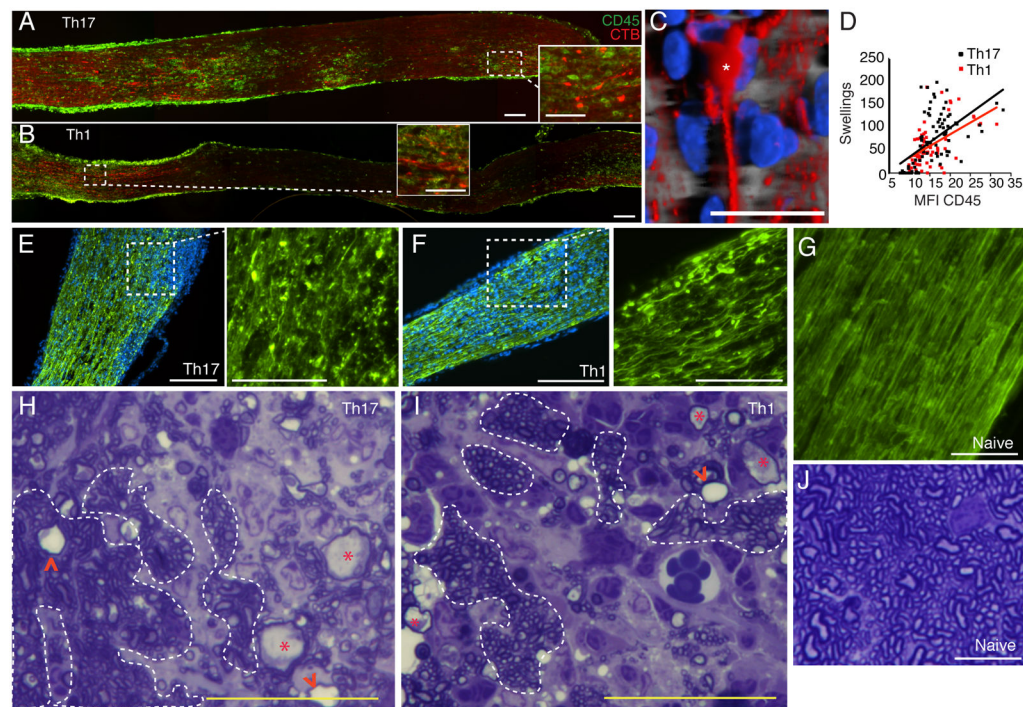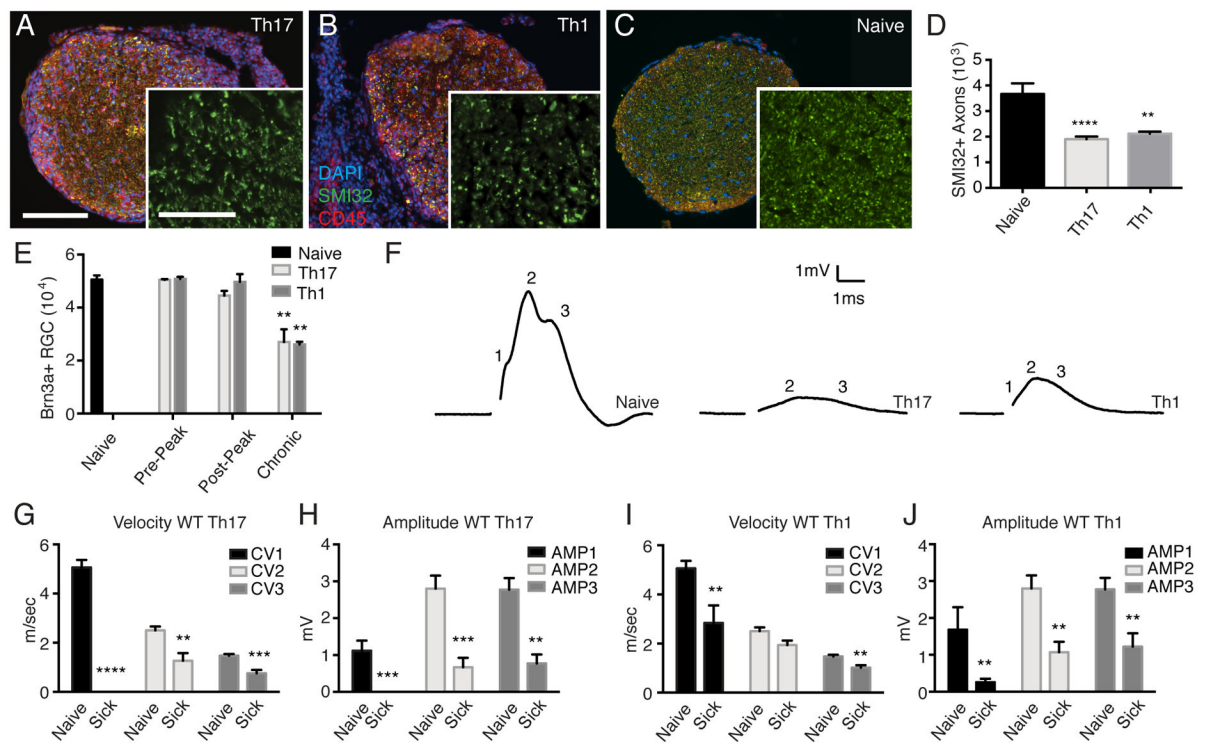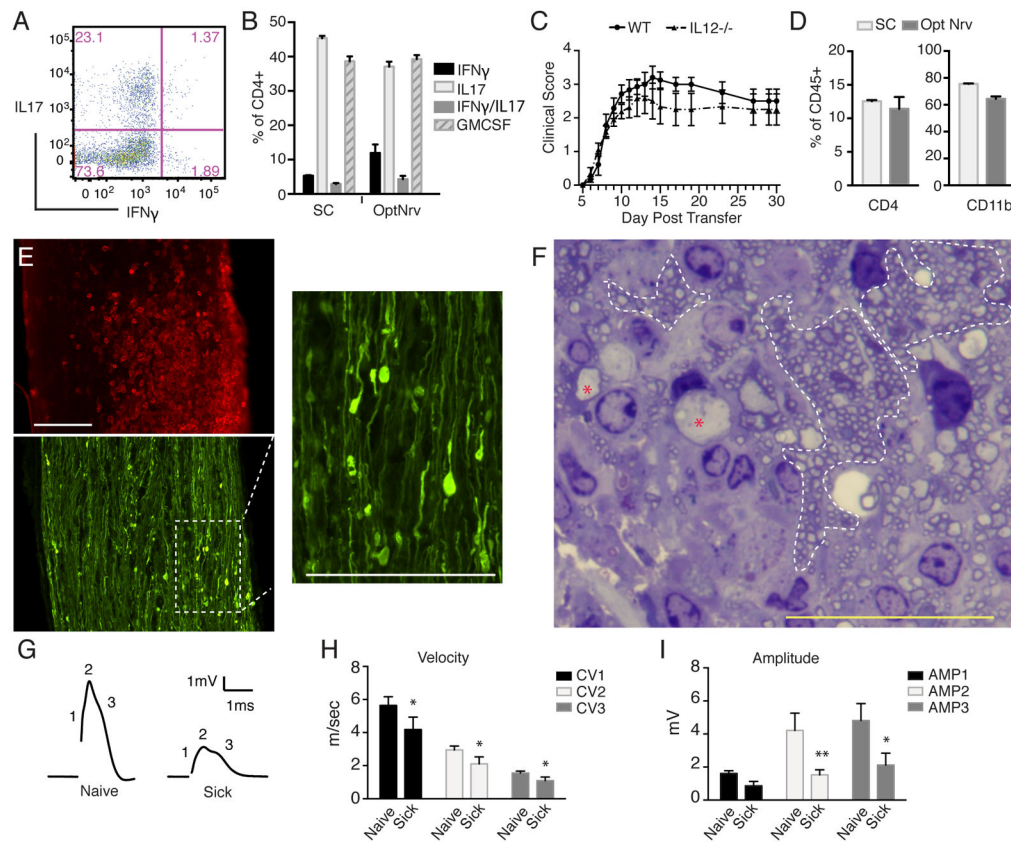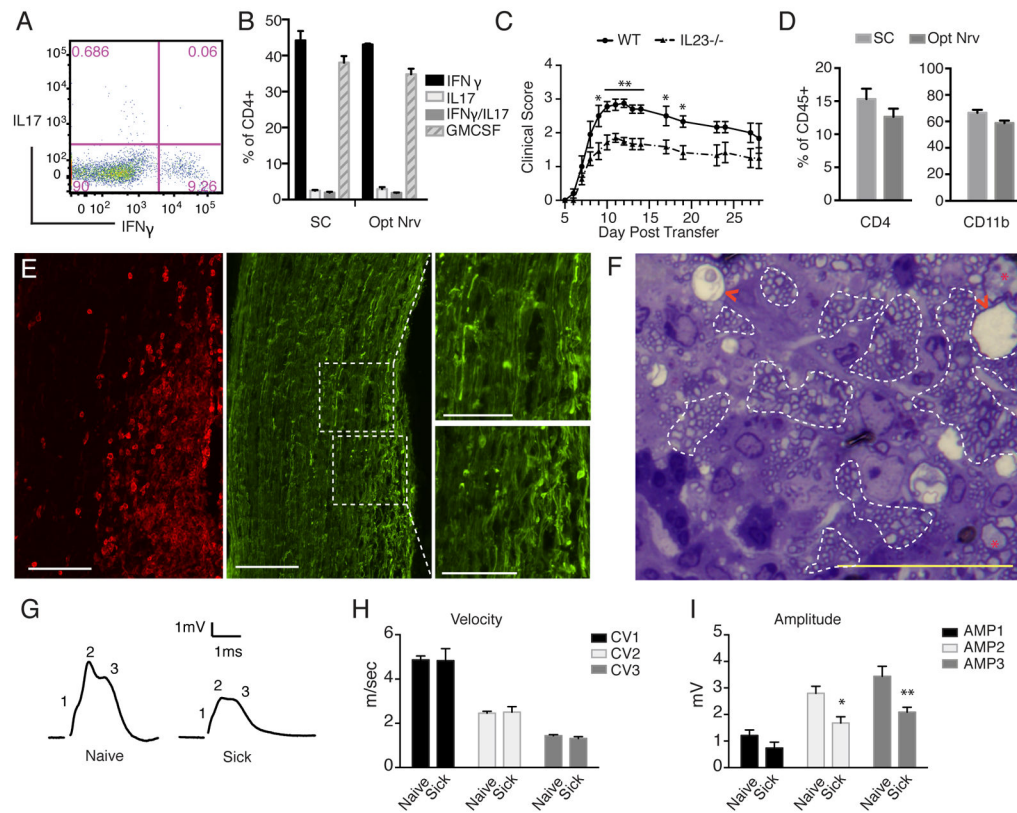
FIGURE 2.
Axonopathy is an early feature of both Th1- and Th17-mediated ON. (**A–D**) Th1 and Th17 adoptive transfer recipients were injected i.o. with fluorochrome-conjugated cholera toxin-B (red) at onset of clinical EAE. Optic nerves were harvested 24 hours later. Longitudinal sections were stained for the pan-leukocyte marker, CD45 (green) to demarcate areas of inflammation. (**C**) Confocal microscopy revealed a swelling at the tip of a transected axon (asterisk). (**D**) The frequency of axonal swellings was compared with the intensity of CD45 staining and there was no significant difference. (**E–G**) Cross- sections of optic nerves harvested from mice with Th17- (**E**) and Th1- (**F**) mediated ON were stained for unphosphorylated neurofilament-H (SMI-32, green; DAPI, blue; bars=50 μm). Magnified views of the insets are shown in adjacent panels (bars=25 μm). (**G**) SMI-32 staining of a healthy nerve (bar= 50 μm). (**H–J**) Representative cross-sections of optic nerves obtained from mice with Th17- (**H**) or Th1-(**I**) mediated ON, or from naïve mice (**J**), were stained with toludine blue. Broken lines delineate representative areas with normal-appearing axons, asteriscs indicate swollen axons and arrowheads point to empty myelin sheaths (bars= 25 μm).
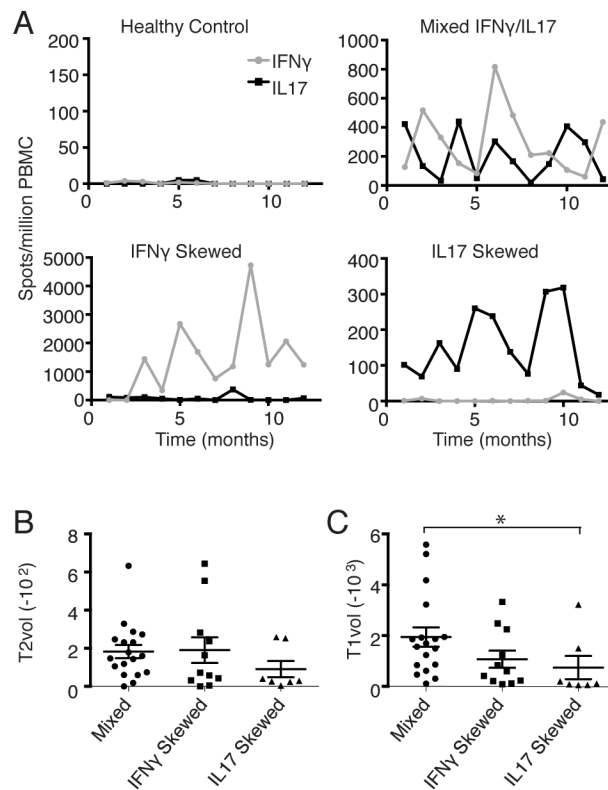
FIGURE 3.
Axon loss and faulty nerve conduction occur in both Th1- and Th17-mediated ON. (**A–D**) Optic nerves harvested immediately before the peak of EAE were stained with antibodies against SMI32 (green) and CD45 (red). Representative cross-sections of nerves from mice with Th17- (**A**) and Th1- (**B**) mediated ON, as well as from a naïve mouse (**B**), are shown (bars = 100 μm and 25 μm, inset) and quantified (**D**). (**E**) Brn3a$^+$ RGCs were counted in retinas harvested from naïve mice, and from ON mice at serial time points post-transfer (t-test). (**F**) Representative traces of CAPs of optic nerves acutely isolated from naïve and ON mice. CAP velocities (**G, I**) and amplitudes (**H, J**) were averaged over seven to twelve nerves per group. Data presented as mean ±S.E.M. (**p<0.01, ***p<0.001, ****p<0.0001; Mann-Whitney) Scale bars: A, B 50μm, insets 25μm; C 25μm.

FIGURE 4.

Stable Th17 cells induce ON. (**A**) Intracellular cytokine production by CD4$^+$ T cells derived from MOG-immunized IL-12KO mice, after 96 hours of culture with MOG$_{35-55}$ and recombinant IL-23. (**B**) Intracellular cytokine production by CD4$^+$ T cells derived from MOG-immunized IL-12KO donors after infiltrating the spinal cords and optic nerves of IL-12KO hosts. (**C**) Clinical courses of IL-12KO mice injected with myelin-specific CD4+ Th17 cells derived from IL-12KO donors versus WT mice injected with WT effector Th17 cells. The data shown is pooled from 3 experiments with n=10 WT and n=17 IL12KO host mice per group. (**D**) The percentage of CD4$^+$ T cells and CD11b$^+$ myeloid cells among CD45$^+$ leukocytes infiltrating the optic nerve and spinal cord of IL-12KO hosts shortly after the onset of clinical EAE. (**E**) Contiguous sections of an optic nerve obtained from an IL-12KO host at clinical EAE onset and stained with CD45 (red, top left panel) or SMI-32 (green). (**F**) A representative section stained with toludine blue (bars= 50μm in D, 25μm in E). Areas with normal appearing axons are outlined, asteriscs indicate swollen axons and arrowheads point to empty myelin sheaths. (**G–I**) CAPs were measured in acutely isolated optic nerves from the IL-12KO recipients of stable Th17 cells at clinical EAE onset. (**G**) Representative wave-forms of optic nerve CAPs from a naïve IL-12KO mouse and an IL-12KO adoptive transfer recipient with acute ON. The data were averaged over seven to nine nerves per group. Data are presented as mean ±S.E.M. (*p<0.05, **p<0.01; Mann-Whitney)

FIGURE 5.

Bona Fide Th1 cells are capable of inducing ON. (**A**) Intracellular cytokine production by CD4$^+$ T cells derived from MOG-immunized IL-23KO mice, after 96 hours of culture with MOG$_{35-55}$ and recombinant IL-12. (**B**) Intracellular cytokine production by CD4$^+$ T cells derived from MOG-immunized IL-23KO donors after infiltrating the spinal cords and optic nerves of IL-23KO hosts. (C) Clinical courses of IL-23KO mice injected with myelin-specific CD4+ Th1 cells derived from IL-23KO donors versus WT mice injected with WT effector Th17 cells. The data was pooled from 3 experiments with n=9 WT and n=22 IL-23KO hosts (*p<0.05, **p<0.01; Holm-Sidak multiple t-tests). (**D**) The percentage of CD4$^+$ T cells and CD11b$^+$ myeloid cells among CD45$^+$ leukocytes infiltrating the optic nerve and spinal cord. (**E**) Contiguous sections of a representative optic nerve obtained from an IL-23KO host at clinical EAE onset and stained with CD45 (red, left panel) or SMI-32 (green, right panels). (**F**) A representative section stained with toluidine blue. (bars= 50μm in E, 25μm in insets and in F). Examples of areas with normal appearing axons are outlined, asterisks mark examples of swollen axons and arrowheads point to myelin sheaths left behind by degenerated axons. (**G–I**) CAPs were measured in optic nerves from the IL-23KO recipients of Th1 cells at clinical EAE onset. The data were averaged over seven to nine nerves per group. (**G**) Representative wave-forms. CAP velocities (**H**) and amplitudes (**I**) were measured in eight to twelve nerves per group. Data are presented as mean ± S.E.M. (*p<0.05, **p<0.01; Mann-Whitney)

FIGURE 6.

MS patients have diverse myelin-specific cytokine profiles. (**A–C**) PBMC were collected from relapsing MS patients with moderate disability on a monthly basis over the course of 1 year. (**A**) ELISPOT assays were performed to assess the frequency of MBP-specific IFNγ and IL-17 producers. Representative examples are shown. Patients were classified into three groups: IFNγ predominant (n=11), IL-17 predominant (n=7) and IFNγ/IL-17 mixed (n=18), based on criteria described in the Materials and Methods section. (**B, C**) Each subject underwent cerebral MRI scanning. T1- and T2-weighted lesion volume and brain parenchymal volume (BPV) were measured using a semi-automated approach [17]. The figures show average T1 and T2 lesion volumes normalized to total BPV. (*p=0.02; non-parametric, one-way ANOVA with Dunn's multiple comparisons test)